JOURNAL OF AGRICULTURAL AND FOOD CHEMISTRY

Photodegradation of Metolachlor Applying UV and UV/H_2O_2

CHANGLONG WU, HILLA SHEMER, AND KARL G. LINDEN*

Department of Civil and Environmental Engineering, Duke University, 121 Hudson Hall Engineering Building, Box 90287, Durham, North Carolina 27708-0287

Metolachlor is one of the most widely used herbicides in the world for controlling weeds. It has been detected in both ground and surface waters in the United States, and there are rising concerns in regard to its health risks and in developing effective treatment processes for its removal from water. Degradation of metolachlor via ultraviolet (UV) photolysis and an UV/hydrogen peroxide advanced oxidation process (AOP) was studied. The quantum yield of metolachlor at 254 nm was found to be 0.302 ± 0.001 mol E^{-1} through direct UV photolysis in the range of pH 6−8. The second-order rate constant of the reaction between metolachlor and hydroxyl radical was determined to be 9.07 ($\pm$0.21) $\times$ 10^9 M^{-1} s^{-1} by using a competition kinetics model that utilized nitrobenzene as a reference compound. In addition, these parameters were successfully applied in modeling the kinetics of elimination of metolachlor using an UV/H_2O_2 process in both laboratory and natural waters. The formation of several photolysis byproducts was identified using gas chromatography/mass spectrometry, and a scheme for the metolachlor photodegradation pathway is proposed.

KEYWORDS: UV irradiation; AOPs; herbicides; chloroacetamides; photolysis; degradation

INTRODUCTION

Metolachlor [2-chloro-*N*-(2-ethyl-6-methylphenl)-*N*-(2-methoxy-1-methylethyl) acetamide], a chloroacetamide herbicide, is among the most widely used herbicides for the control of grasses in crops, such as soybeans, corn, and beans. The use of metolachlor has increased steadily, and it recently replaced alachlor as the major acetamide herbicide. However, according to the U.S. EPA, the consumption of metolachlor in the United States decreased from 59 to 67 million lbs in 1997 to 15−22 million lbs applied in 2001 (*1*).

Like other widely used chloracetamide herbicides (alachlor, butalochlor, and acetochlor), metolachlor is partially degraded in anaerobic wetlands with a half-life of 40−62 days (*2*). It is rather stable under natural sunlight and corn field conditions with a half-life ranging from 21 to 205 days (*3*, *4*). Because of its high water solubility (530 mg L^{-1} at 20 °C) and low K_{ow} (octanol−water partition coefficient) value (indicating high mobility), metolachlor has the potential to contaminate surface and groundwaters. It has been detected in shallow groundwaters of 20 major basins in the United States with a maximum concentration of 5.4 μg L^{-1} (*5*) and surface waters with concentration ranges from 0.1 to tens of μM (*6*). Because of its moderate toxicity and potential carcinogenic effects, metolachlor was included in the 1998 and 2005 U.S. EPA Candidate Contaminant Lists. The World Health Organization established in its guidelines a health-based value of 10 μg L^{-1} for metolachlor in drinking water (*7*). A higher value of 50 μg L^{-1} defined as an Interim Maximum Acceptable Concentration was regulated by the Canadian Drinking Water Standard (*8*).

There has been considerable research on the microbial and chemical degradation of metolachlor in aqueous environments. Metolachlor can be extensively transformed by microorganisms, and several metabolites have been identified using GC/MS (gas chromatography/mass spectroscopy) and nuclear magnetic resonance spectroscopy methods in which metolachlor ethane sulfonic acid (ESA) and metolachlor oxanilic acid (OA) were the two most common metabolites (*9*). Kalkhoff et al. (*10*) showed that ESA and OA were generally present 3−45 times more frequently as compared to their parent compound. Acero et al. (*11*) studied the oxidation of metolachlor by ozone and by the combination of ozone/hydrogen peroxide (H_2O_2) and reported a k_{OH} [rate constant for the reaction of metolachlor with hydroxyl (OH) radicals] value of 6.9×10^9 M^{-1} s^{-1}. Pignatello and Sun (*9*) reported that metolachlor undergoes considerable degradation in the photo-assisted Fenton reaction. The attack of OH radical was nonspecific and occurred on the ring, ring alkyl group, and amide alkyl group. Kochany and Maguire (*3*) studied the sunlight photodegradation of metolachlor and reported four photodegradation products. Monochloroacetic acid (MCA) was identified as the major product of sunlight photodegradation of metolachlor (*13*). In addition, a study on the UV degradation of metolachlor under 254 nm irradiation in water in the presence of soil mineral and organic constituents yielded five photolysis products: (2-hydroxy-*N*-2-ethyl-6-methylphenyl)-*N*-(2-methoxy-1-methylethyl) acetamide; 4-(2-ethyl-6-methylphenyl)-5-methyl-4-morpholine; 8-ethyl-3-hydorxy-*N*-(2-methoxy-1-methylenyl)-2-oxo-1,2,3,4-tetrahydroquinoline; 2-chloro-*N*-[2-(1-hydroxyethyl)-6-

* To whom correspondence should be addressed. Tel: +1-919-660-5196. Fax: +1-919-660-5219. E-mail: kglinden@duke.edu.

10.1021/jf0635762 CCC: $37.00
Published on Web 04/21/2007

methylphenyl]-*N*-(2-hydroxy-1-methylethly) acetamide; and 2-chloro-*N*-(2-ethyl-6-hydroxymethylphenyl)-*N*-2-methoxy-1-methylethyl) acetamide (*14*). Although photodegradation has been shown to occur, metolachlor is relatively resistant to photolytic decomposition (*3*). Beyond photolysis, there is little information in the literature on the physicochemical fate of metolachlor in aquatic systems. Metolachlor is resistant to hydrolysis, and because of its low volatility [Henry's law constant $K_H = 42.6\ (\pm 2.8) \times 10^3$ (M atm^{-1}) at 293 K (*13*, *15*)], air striping is not effective. Thus, both photolysis and oxidation processes are the most likely techniques to be viable for the treatment of water contaminated with metolachlor.

Two promising approaches for degradation of metolachlor in a water treatment system are UV photolysis, such as that used in disinfection, and the combination of UV irradiation with an oxidizing agent, such as H_2O_2. The process involves both direct UV photolysis (governed by the absorption spectra of target compounds and quantum yield) as well as the reactions between target compounds and OH radicals, which are generated by the photolysis of H_2O_2 via absorption of UV light in a wavelength range of 200−300 nm. OH radicals can oxidize nearly all organic compounds by abstracting a hydrogen atom, adding OH groups, and electron transfer (*16*). The UV/H_2O_2 process was successfully applied for the degradation of various organic contaminants such as endocrine disrupting chemicals, benzene, MTBE, NDMA, and nitroaromatics (*17*−*20*).

The purpose of this study was to evaluate photodegradation properties of metolachlor using a low-pressure UV lamp typical of water treatment systems. Quantum yield, OH radical reaction rate constant, and the basic photodegradation kinetics were determined. A general kinetic model was developed describing the relationship between the rate constant, the H_2O_2 dose, and the water quality parameters. The kinetic model was also validated by predicting metolachlor destruction in natural surface waters. Photodegradation pathways of metolachlor were proposed based on the identification of several byproducts using GC/MS.

MATERIALS AND METHODS

Chemicals. Metolachlor (98.7%) was obtained from Syngenta Co. Ltd. as a solid and was used without further purification. H_2O_2 (30%), high-performance liquid chromatography (HPLC) grade acetonitrile, and water were purchased from Fisher Chemicals. Suwannee River natural organic matter (NOM) was obtained from the International Humic Substances Society. All other reagents used in the study were analytical grade and used as received.

Photolysis Experiments. UV irradiation was carried out using a 15 W germicidal low-pressure UV lamp (ozone-free, General Electric #G15T8) at ambient temperature. The setup was previously described by Rosenfeldt and Linden (*20*). Incident irradiance was determined by a calibrated radiometer (IL1700, SED 240/W, International Light, Peabody, MA). In a typical photolysis experiment, metolachlor was spiked into 120 mL of 0.02 M phosphate buffer solution (PBS) in a 70 mm × 50 mm crystallization dish (the surface area was 34.2 cm^2, and the solution depth was 3.51 cm) and exposed to UV irradiance under completely mixed batch conditions. Initial metolachlor concentrations used in the study varied from 2 to 30 μM. UV fluence was determined from the average 254 nm irradiance as calculated with a spreadsheet program using the lamp spectrum, solution absorbance, exposure time, and the irradiance reading from the calibrated radiometer. At specific delivered UV fluence intervals, a 0.6 mL sample was taken by syringe and was then stored in HPLC vials. A maximum of 3 mL was removed throughout each exposure experiment, minimally affecting the solution volume and depth. Each experiment was performed twice to ensure the repeatability of the data. H_2O_2-assisted photodegradation was studied by adding 5−250 mg L^{-1} H_2O_2 to a PBS solution of metolachlor at pH 7. Only minor dilution of this concentration occurred from the addition of varying concentrations of H_2O_2. Dark controls were conducted, under an identical experimental setup, to ensure that no loss of the metolachlor occurred via processes other than photolysis (i.e., hydrolysis or evaporation).

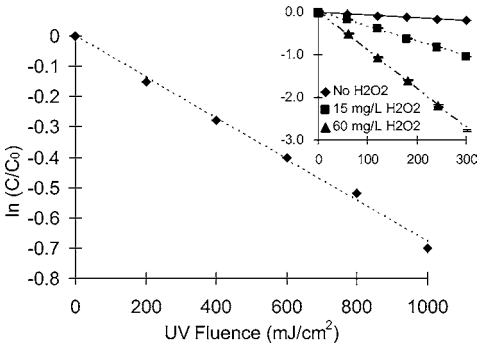

Figure 1. Direct photolysis of metolachlor ([MET] = 30 μM, pH 7.0, T = 20 °C). The insert shows direct and H_2O_2-assisted photolysis.

Analytical Methods. Varian Pro Star HPLC (Varian, Inc., Palo Alto, CA) equipped with a polychromatic diode array detector and C18 reverse phase column (7.5 mm × 150 mm) was used to monitor the concentration of metolachlor by direct injection (50 μL injection volume). Isocratic elution was used with a mobile phase of acetonitrile and water (65/35 v/v) at a flow rate of 1 mL min^{-1}. Under the conditions described above, the retention time (RT) for metolachlor was 7.0 min. Absorbance spectra were measured using a UV spectrophotometer- Cary Bio100 (Varian, Inc.). Total organic carbon was measured by a Tekmar Dohrmann Apollo 9000 Total Carbon analyzer in accordance with Standard Method 5310A (*21*). Residual H_2O_2 was determined by the I_3^- method (*22*). The solution pH was determined by using a Thermo Orion 920A pH meter. Alkalinity was measured according to the Standard Method 2320 (*21*).

Photolysis byproducts of metolachlor were identified using Shimadzu GC/MS-QP5050A gas chromatograph with a 15 m RTX-5 MX column (film thickness, 0.25 μm; i.d., 0.25 mm). Helium was used as the carrier gas, with a flow rate of 1.1 mL min^{-1}. The GC temperature condition was as follows: initial temperature at 80 °C, 10 °C/min gradient until 250 °C, 3 min final hold. The detector temperature was 280 °C. The electron energy for the EI mass spectrum was 70 eV, and the scan range was 50−400 amu.

Extraction Procedure. For the identification of reaction products, aqueous metolachlor solutions (before and after exposure to UV) were extracted using either liquid−liquid extraction (LLE) or solid-phase extraction (SPE). In the LLE, 60 mL of the aqueous sample was acidified to pH 3 with concentrated sulfuric acid and mixed twice with 6 mL of dichloromethane in a separatory funnel. The extracted phase was passed through an anhydrous sodium sulfate column. The SPE was conducted with Varian Abselut Nexus cartridges (100 mg) by passing 60 mL of aqueous samples through the cartridge at flow rate of 2 mL min^{-1}. The cartridge was then washed twice with 5 mL of methanol. The extracts in both procedures were concentrated to about 0.7 mL by evaporation using a gentle stream of nitrogen at 40 °C, and internal standards and surrogates were added in the solution as volumetric standards prior to GC/MS analysis. The identification of the photodegradation byproducts was confirmed by comparing RT as well as *m*/*z* values of available authentic samples and the interpretation of *m*/*z* charts.

RESULTS AND DISCUSSION

Direct Photolysis and Quantum Yield. Photodegradation of metolachlor exhibited pseudo-first-order kinetics, with a rate constant (k_d) of 7.25 ($\pm$0.04) × 10^{-4} cm^2 mJ^{-1}, at pH 7. Approximately half of the metolachlor was transformed at UV fluence of 1000 mJ cm^{-2} (**Figure 1**).

Quantum yield (Φ) and molar absorption are two fundamental parameters that govern the rate of direct photodegradation.

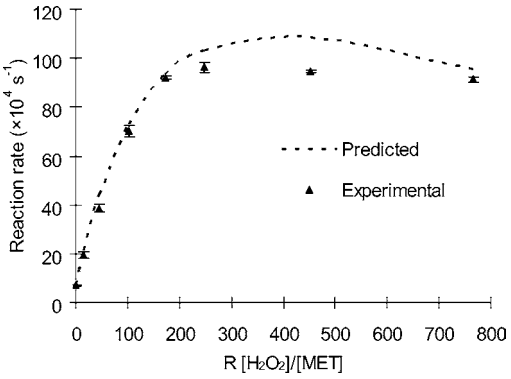

Figure 2. Comparison of the predicted (line) and experimental (dots) reaction rates of metolachlor at various molar ratios of H_2O_2 to metolachlor.

The overall photolysis rate and the quantum yield were calculated using eqs 1 and 2 (*23*).

$$-\frac{\mathrm{d[MET]}}{\mathrm{d}t} = k\,\mathrm{d[MET]} = k_{\mathrm{S,MET}}\,\Phi_{\mathrm{MET}} \tag{1}$$

$$\Phi_{\mathrm{MET}} = \frac{k_{\mathrm{d}}}{k_{\mathrm{S,MET}}} \tag{2}$$

where Φ_{MET} is the quantum of metolachlor; k_d is the pseudo-first-order reaction rate constant; $K_{S,MET}$ is the specific rate of light absorption by metolachlor (E mol^{-1} s^{-1}), in which $k_{S,MET} = E_P^0\epsilon_{MET}[1 - 10^{-aZ}]/aZ$; E_P^0 is the incident photon irradiance (10^{-3} E cm^{-2} s^{-1}); ϵ_{MET} is the molar absorbance of metolachlor (M^{-1} cm^{-1}), measured as 503 M^{-1} cm^{-1} at $\lambda = 254$ nm; a is the solution absorbance at wavelength 254 nm; and Z is the solution depth.

The quantum yield of metolachlor (at 254 nm) was found to be 0.302 ± 0.001 mol E^{-1} at pH values between 6 and 8, which corresponds to most natural water pH levels. This value is approximately half of the previously reported average value of 0.56 ± 0.05 mol E^{-1}, evaluated through a competitive kinetic model that utilized the simultaneous photochemical oxidation of mixtures of metolachlor and propachlor at pH values of 2, 5, 7, and 9 (*24*). It is also noteworthy that the quantum yield reported by Kochany and Maguire (*3*), $5.6-9.6 \times 10^{-3}$ mol E^{-1}, is about 30 times lower than the value found in this study. The discrepancy between these results is likely due to the different wavelength studied, 254 nm as compared to the UVA and UVB wavelengths of between 280 and 330 nm used in their work.

UV/H_2O_2 Advanced Oxidation. Degradation of metolachlor by the UV/H_2O_2 advanced oxidation process (AOP) is via reaction with OH radicals, produced by UV irradiation of H_2O_2. H_2O_2 was added to the metolachlor solutions at concentrations from 5 to 250 mg L^{-1} (corresponding to 1.5×10^{-4} to 7.3×10^{-3} M). As expected, the destruction of metolachlor increased significantly using UV combined with H_2O_2 as compared to its direct photolysis, as shown in **Figure 1**. It can be concluded that the reaction between the OH radicals formed and the metolachlor was the major destruction pathway.

The reaction rates of metolachlor at various molar ratios between H_2O_2 and metolachlor are shown in **Figure 2**. The destruction rates initially increased upon increasing the molar ratio of H_2O_2 to metolachlor up to an optimal rate obtained at a molar ratio of approximately 200, after which the reaction rate remained constant (**Figure 2**). A similar trend was also observed for UV/H_2O_2 degradation of 1,2-dibromo-3-chloropropane, acetone, and nitroaromatics (*18*, *25*, *26*). Several competing effects may contribute to obtaining an optimal rate of degradation as a function of the molar ratio of H_2O_2 to metalochlor (**Figure 2**). First, with an increasing concentration of H_2O_2, more OH radicals are produced and hence available for the destruction of metolachlor (eq 3)

$$H_2O_2 + h\nu \rightarrow 2OH^{\bullet} \tag{3}$$

Second, the reaction between H_2O_2 and OH radicals that produces $HO_2^{\bullet}$, which are much less reactive as compared to OH radicals, becomes significant at a higher concentration of H_2O_2; thus, the H_2O_2 acts as a OH radical scavenger (eq 4):

$$H_2O_2 + {}^{\bullet}OH \rightarrow HO_2^{\bullet} + H_2O \tag{4}$$

Third, the higher concentration of H_2O_2 may effectively absorb UV light and provide a screening effect that reduces the photodecomposition of metolachlor (*18*, *27*). Because of these effects, an optimal H_2O_2 concentration exists, which represents the optimum between the competition of UV light absorbance and the reaction between OH radicals.

The steady-state concentration of OH radicals in solution can be expressed by the ratio between the production rate and the depletion rate of OH radicals (eq 5).

$$[{}^{\bullet}OH]_{SS} = \frac{R_{p,OH}}{R_{S,OH}} = \frac{R_{p,OH}}{\sum k_i[s_i]} = \frac{k_{S,H_2O_2}\,\Phi_{H_2O_2}\,[H_2O_2]\,f_{H_2O_2}}{k_{H_2O_2}\,[H_2O_2] + k_{MET}\,[MET]} \tag{5}$$

where $[{}^{\bullet}OH]_{SS}$ is the steady-state concentration of OH radicals; $R_{p,OH}$ is the production rate of OH radicals; $R_{S,OH}$ is the sum of the scavenging rate of OH radicals; $k_{H_2O_2}$ is the rate constant between OH radicals and H_2O_2 ($k_{H_2O_2} = 2.7 \times 10^7$ M^{-1} s^{-1}) (*28*); $f_{H_2O_2}$ is the fraction of UV absorbed by H_2O_2 (eq 6):

$$f_{H_2O_2} = \frac{\epsilon_{H_2O_2}\,[H_2O_2]}{\epsilon_{H_2O_2}\,[H_2O_2] + \epsilon_{MET}\,[MET]} \tag{6}$$

and k_{S,H_2O_2} is the specific rate of light absorption by H_2O_2 (E mol^{-1} s^{-1}). The fraction of photons absorbed by the H_2O_2 nonlinearly increases with the increasing of H_2O_2 concentration (eq 6). In fact, in the presence of high concentrations of H_2O_2, photon absorbance by metolachlor is negligible. On the other hand, the scavenging effect expressed by the denominator in eq 5 also increases with increasing H_2O_2 concentration. The combination of these effects causes the steady-state concentration of OH radicals to increase at low concentrations of H_2O_2 and remain constant or decrease slightly at higher concentrations of H_2O_2. **Figure 3** shows the fraction of photons absorbed by metolachlor and H_2O_2, respectively (left axis). Also shown is the calculated concentration of OH radicals from eq 5, which varied from 1 to 12×10^{-13} (M) (right axis). Given that the reaction between OH radicals and metolachlor dominates the destruction of metolachlor in the UV/H_2O_2 process, the destruction rate of metolachlor should follow a trend similar to the concentration of OH radicals at different doses of H_2O_2. Thus, the rate of degradation of metolachlor can be predicted accurately at various molar ratios of H_2O_2 to metolachlor as shown in **Figure 2**. The difference between the predicted and the experimental dependence of degradation rate on the molar ratio of metolachlor to H_2O_2 beyond 200 may be due to formation of the less reactive secondary radicals at high H_2O_2 concentra-

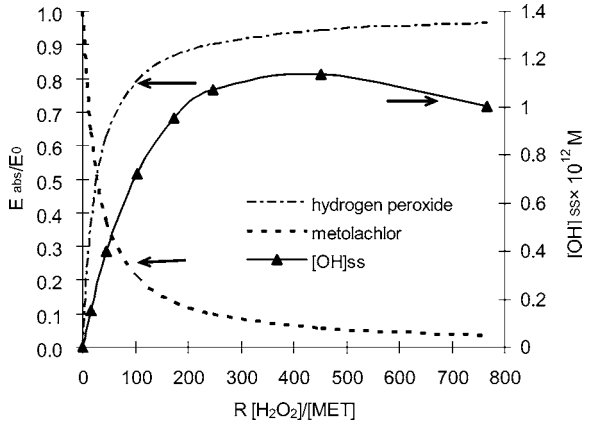

Figure 3. Fractions of light absorbed by H_2O_2 and metolachlor and steady-state concentration of OH radicals at various molar ratios between H_2O_2 and metolachlor.

Table 1. Comparison of Predicted and Experimental Destruction Rates of Metolachlor at Various Concentrations of NOM and H_2O_2

H_2O_2 (mg L^{-1})	NOM (mg L^{-1} DOC)	k_{obs} ($\times 10^3$ s^{-1})	k_{mod} ($\times 10^3$ s^{-1})	differences (%)
25	1.57	6.35	6.41	1.04
25	3.14	4.33	3.92	9.60
25	4.71	2.73	2.72	4.24
50	1.57	8.60	9.15	6.39
50	3.14	5.59	5.75	2.98
50	4.71	3.87	3.94	1.82

tions (such as $HO_2^{\bullet}$, as presented in eq 4), which are not taken into account during calculation of the predicted values.

OH Radical Rate Constant. Competition kinetics experiments were conducted to evaluate the rate constant (k_{OH}) between OH radicals and metolachlor (*18*, *29*). Nitrobenzene [$k_{OH} = 4.0 \times 10^9$ M s^{-1} (*28*)] was chosen as the reference compound because it essentially does not undergo direct photolysis, it is easy to analyze using HPLC, and it has been successfully applied in similar experiments (*30*). Most previous studies on the UV/H_2O_2 process assumed that the direct photolysis of the target compounds was negligible (*20*, *31*). However, as discussed above, because of the high quantum yield, metolachlor undergoes considerable direct photolysis. Such an effect should be taken into consideration in determining the OH radical rate constant via a UV-based process. Noting that the direct photolysis of nitrobenzene is negligible, the destruction rates of metolachlor and nitrobenzene can be expressed by eqs 7 and 8, respectively.

$$r_{MET} = k_{OH,MET}[^{\bullet}OH]_{SS} + k_{s,MET}\,\Phi_{MET}\,f_{MET} \quad (7)$$

$$r_{NB} = k_{OH,NB}[^{\bullet}OH]_{SS} \quad (8)$$

Here, the steady-state concentration of OH radicals was calculated according to eq 5 where the composition of $\sum k_i[s_i]$ also included the degradation rate of the NB ($k_{H_2O_2}[H_2O_2] + k_{MET}$ [MET] + k_{NB} [NB]), and the fraction of UV absorbed by metolachlor (f_{MET}) was determined by eq 9.

$$f_{MET} = \frac{\epsilon_{MET}\,[MET]}{\epsilon_{H_2O_2}\,[H_2O_2] + \epsilon_{NB}\,[NB] + \epsilon_{MET}\,[MET]} \quad (9)$$

Thus, the reaction rates for both metolachlor and nitrobenzene can be calculated from the changes in their concentrations as a function of UV fluence. Because nitrobenzene shows little direct photolysis under the experimental conditions (data not shown), the OH radical rate constant of metolachlor can be calculated using eq 10.

$$k_{OH,MET} = k_{OH,NB}\frac{r_{MET} - k_{S,MET}\,\Phi_{MET}\,f_{MET}}{r_{NB}} \quad (10)$$

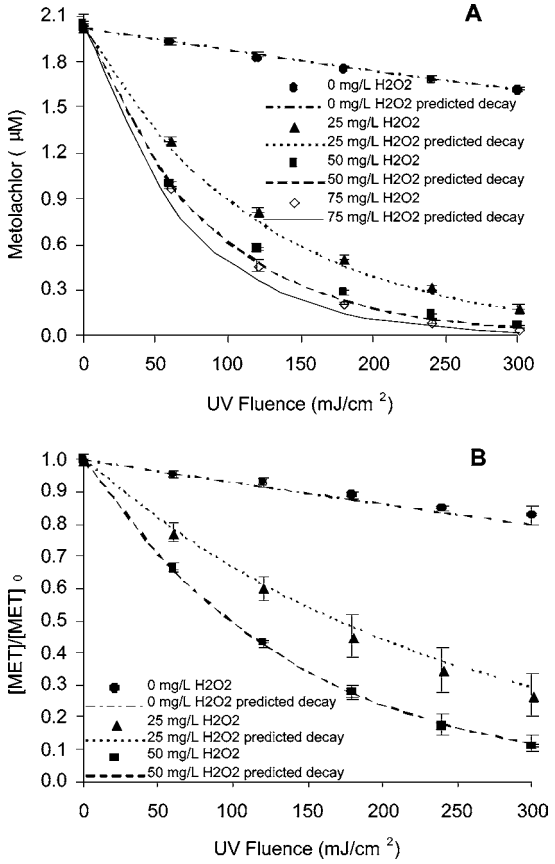

Figure 4. Comparison of predicted (line) and experimental (dots) destruction of metolachlor at various concentrations of H_2O_2: (**A**) PBS, [DOC] = 0.96 mg L^{-1} and alkalinity = 100 mg L^{-1} as $CaCO_3$; (**B**) Eno River water, [DOC] = 5.78 mg L^{-1} and alkalinity = 23 mg L^{-1} as $CaCO_3$.

The above equations were applied for experimental data obtained at various initial concentrations of H_2O_2, metolachlor, and nitrobenzene. The OH radical rate constant of metolachlor was found to be constant using the various concentrations, and an average value of 9.07 ($\pm$0.21) $\times 10^9$ M^{-1} s^{-1} was obtained and used for subsequent studies. This value compares well with the value of 6.7 ($\pm$0.4) $\times 10^9$ M^{-1} s^{-1}, obtained in a study of ozone/H_2O_2 treatment of metolachlor (*11*).

Scavenging Effects of DOC and Alkalinity. AOP processes that utilize the reaction between OH radicals and substrates are subject to scavenging effects because OH radicals are nonselective and can react with virtually any species present in aqueous solutions ($E_0 = 2.8$ V; *32*). Carbonate species (HCO_3^-, CO_3^{2-}), NOM, and H_2O_2 can act as OH radical scavengers and hence reduce the destruction rate of metolachlor. The effects of these scavenging species were investigated at pH 7, 20 °C with 2 μM metolachlor, and a range of 0−50 mg L^{-1} of H_2O_2. In the presence of NOM and carbonate species, the expression of steady-state OH radical concentration (eq 5) was modified; thus, the denominator included the

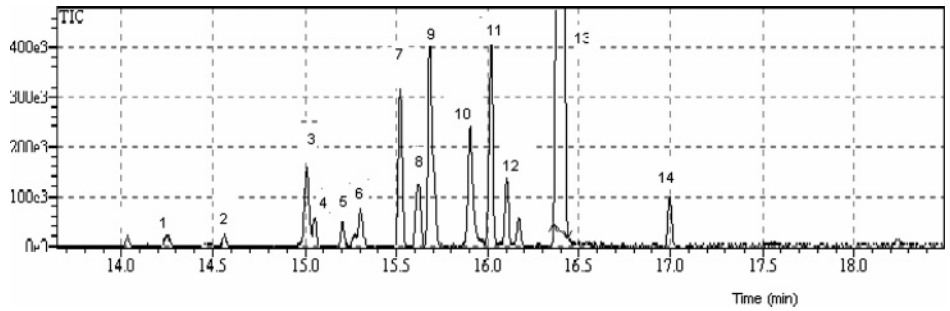

Figure 5. Typical GC/MS chromatogram of the photolysis experiments ([MET] = 25 μM, pH 7.0, UV fluence of 1000 mJ cm^{-2}).

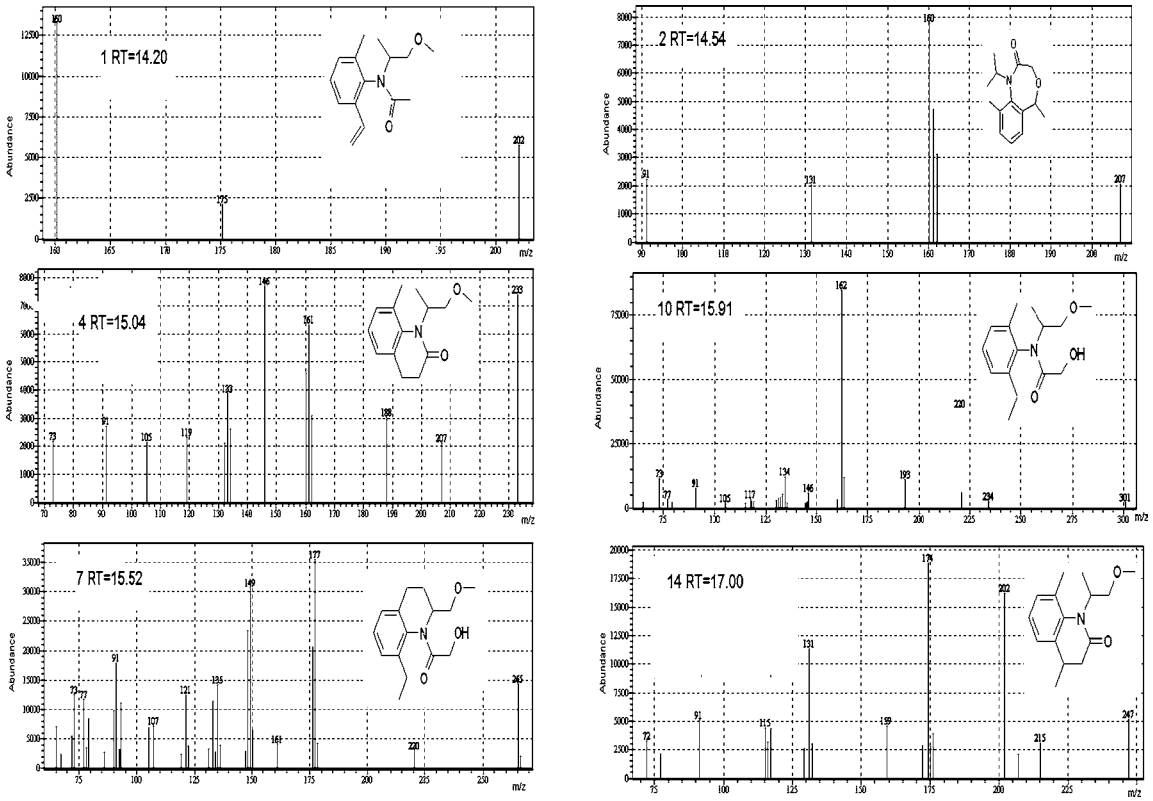

Figure 6. Mass spectra and proposed structures of six byproducts.

scavenging rates of bicarbonate, carbonate, NOM, and H_2O_2, respectively (eq 11).

$$[^{\bullet}OH]_{SS} = \frac{R_{p,OH}}{R_{S,OH}} = \frac{R_{p,OH}}{\sum k_i[s_i]} = \frac{K_{S,H_2O_2}\,\Phi_{H_2O_2}\,[H_2O_2]\,f_{H_2O_2}}{k_{HCO_3^-}[HCO_3^-] + k_{CO_3^{2-}}[CO_3^{2-}] + k_{NOM}[NOM] + k_{H_2O_2}[H_2O_2]} \quad (11)$$

where $k_{HCO_3^-} = 8.5 \times 10^6$ M^{-1} s^{-1}; $k_{CO_3^{2-}} = 3.9 \times 10^8$ M^{-1} s^{-1}; and $k_{NOM} = 2.5 \times 10^4$ mg L^{-1} s^{-1} (*33*).

An increase of the NOM concentrations from 1.6 to 4.7 mg L^{-1} C resulted in a decrease of the destruction rate of metolachlor (**Table 1**). The predicted values of the destruction rate of metolachlor using eqs 7 and 11 (k_{mod}) at various NOM concentrations were found to be in good correlation with the experimental results (k_{obs}) for initial H_2O_2 concentrations of both 25 and 50 mg L^{-1}, as shown in **Table 1**. Carbonate/bicarbonate decreased the degradation rate of metolachlor but to a much lesser extent as compared to NOM (data not shown). **Figure 4A**, which includes several sets of near identical experiments, displays the combined effects of NOM, carbonate species, and H_2O_2. The predicted values of the destruction rate of metolachlor were accurate at lower initial H_2O_2 concentrations up to 50 mg L^{-1}, yet overestimated at higher H_2O_2 levels. Such discrepancy is typical mainly because the OH radical and NOM rate constants used simplify the diverse composition of functional groups for different types of NOM. Nonetheless, this model proved effective in predicting the destruction of metolachlor with an average difference between the predicted and the experimental rate constant of about 5%.

The accuracy of the model was further verified in a natural water system. **Figure 4B** presents the experimental and predicted degradation of metolachlor in a natural water obtained from the Eno River in Durham, NC. Water quality parameters (summarized in the caption of **Figure 4B**) such as DOC and carbonate species were integrated in the model (eq 11) in order to characterize the scavenging effect of the natural water. The predicted degradation of metolachlor agreed well with the experimental results at H_2O_2 concentrations ranging from 0 to 50 mg L^{-1}.

Table 2. GC/MS RTs and Fragmentation Patterns of Unresolved Byproducts

compounds	RT	ions (*m*/*z*) and abundance
3	15.01	247 (1), 233 (30), 203 (13), 202 (100), 175 (62), 174 (82), 161 (36), 160 (55), 146 (52), 132 (15), 91 (28), 77 (17)
5	15.21	247 (45), 202 (11), 176 (7), 131 (100), 117 (27), 91 (32), 73 (86)
6	15.31	202 (100), 175 (82), 174 (92), 160 (59), 146 (18), 91 (7)
9	15.69	265 (7), 247 (24), 202 (43), 175 (56), 174 (100), 160 (21), 146 (18)
11	16.01	248 (3), 247 (23), 202 (42), 175 (59), 174 (100), 160 (11), 146 (27), 146 (27)
12	16.11	232 (7), 215 (55), 202 (94), 176 (35), 174 (66), 160 (43), 159 (26), 132 (25), 131 (100), 117 (23), 91 (26), 72 (35)

Photodegradation Byproduct Identification. During UV disinfection of water via photolysis or natural photodecay in the environment, unwanted degradation products may be formed from parent compound destruction. Because direct photolysis of metolachlor is significant, the formation of intermediate photodegradation products was assessed under UV irradiation. Direct photolysis of metolachlor, at initial concentrations of 25−30 μM and pH 7, resulted in the formation of several intermediates, of which most were eluted before the metolachlor (RT, 16.4 min). **Figure 5** is a typical GC/MS chromatogram of the solution following photolysis of metolachlor obtained after LLE extraction. Dechlorination, hydroxylation, oxoquinoline formation, and demethylation were the processes observed during the photolysis of metolachlor. Compound **13**, with MW of 283, corresponds to the parent metolachlor, which was verified with a metolachlor standard. The mass spectrum of this peak (UV treated extracted sample) showed major ion peaks at *m*/*z* 162, 238, and 240; the latter is of one-third relative abundance of the ion peak of *m*/*z* 240. The ion peak of *m*/*z* 238 may have resulted from the loss of CH_3OCH_2 group, and the ion peak of *m*/*z* 240 indicates the presence of chlorine atom. As compared with the standard mass spectrum of metolachlor, the probability of this compound corresponding to metolachlor is 98%. The identification of other compounds, shown in **Figure 5**, was tentative, and hence still required further investigation or other analytical methods unless confirmed by authentic samples.

Of all of these byproducts, noted on the chromatogram in **Figure 5**, four could be positively identified upon comparing their electron impact MS fragmentation patterns with those from the literature (**Figure 6**). Thus, compound **1** was identified as *N*-(2-ethyl-6-methylphenyl)-*N*-(2-vinyl-6-methyl)-(*N*-2-hydroxy-1-methylethyl) acetamide ($C_{15}H_{21}NO_2$, MW 247). The molecular ion could lose a CH_2OCH_2 group to give the ion at *m*/*z* 202, which could lose CH_2 and CO groups to give the base ion peak at *m*/*z* 160 (*3*). Compound **2**, which possesses a 5% parent ion at *m*/*z* 233, may correspond to the molecular formula $C_{14}H_{19}NO_2$. The molecular M^+ could lose CH_2O and CH_2 groups to give the peak at *m*/*z* 188, which may lose additional CH_2 and O through γ-rearrangement to give the base ion peak at 160 (*3*). Compound **2** matches with the spectra of the metolachlor metabolite "G" reported by Liu et al. (*9*). Compound **4** (RT, 15.04 min) was identified as 8-methyl-*N*-(2-methoxyl-1-methylethyl)-2-oxo-1,2,3,4,-tetrahydroquinoline ($C_{14}H_{19}NO_2$) with MW 233, compound "VI" reported by McGahen et al. (*34*). The molecular ion could lose CH_3 to give the ion at *m*/*z* 218 and CH_2O to give the ion at *m*/*z* 188. The base ion peak at *m*/*z* 146 is the result of loss of CH_2 from the methyl group.

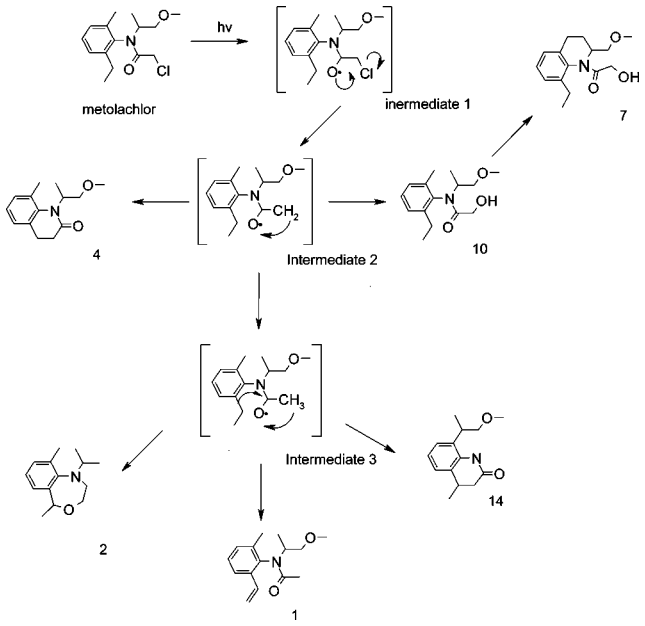

Figure 7. Suggested scheme for photodegradation of metolachlor.

Compound **10**, which gives a fragmentation pattern similar to the sunlight photodegradation product "#1" reported by Kochany and Maguire (*3*), was identified as [2-hydroxy-*N*-(2-ethyl-6-methylphenyl)-*N*-(2-methoxy-1-methylethyl) acetamide] ($C_{15}H_{23}NO_3$). The molecular ion could lose the CH_2OCH_3 fragment to give an ion peak at *m*/*z* 220, while the ion peak at *m*/*z* 193 may result from cleavage of the 2-methoxy-1-methylethyl fragment with hydrogen migration. The ion peak at 220 may lose the $COCH_2OH$ fragment with hydrogen migration to give the base ion peak at *m*/*z* 162.

Two compounds (compounds **7** and **14** in **Figure 6**), whose structures have not been previously reported in the literature, were identified through analysis of the MS spectra. Compound **7** has strong M^+ peak with a molecular weight of 265 ($C_{15}H_{23}NO_3$) with no indication of a chlorine moiety. During the MS process, it may lose the CH_2OCH_3, CH_2, and CH_2OH groups consequently to form the base peak at *m*/*z* of 177. The remaining CO group may also be lost to produce the peak of *m*/*z* 149. Compound **14** (RT, 16.97 min), which has a parent ion at *m*/*z* 247, may correspond to 8-methyl-*N*-(2-methoxy-1-methylethyl)-2-oxo-4-methyl-1,2,3,4,-tetrahydroquinoline ($C_{15}H_{21}NO_2$) with a molecular weight of 247. The molecular ion may lose CH_3OH though hydrogen migration to give an ion peak at *m*/*z* 215 and then lose additional CH to give the ion peak at *m*/*z* 202. It may lose two CH_2 groups to give the base ion peak at *m*/*z* 174. Several byproducts remained unresolved based on current information. **Table 2** summarizes the *m*/*z* peaks and abundance of these byproducts.

Pignatello and Sun (*12*) found that several major byproducts through photo-assisted Fenton reactions of metolachlor retain a chlorine atom, while Kochany and Maguire (*3*) reported dechlorination to be the first step during sunlight photodegradation of metolachlor since none of their identified byproducts contained a chlorine atom. In this study, no chlorine ion was detected by the EI implying that none of the photolysis products contained chlorine. Hence, it can be concluded that dechlorination is one of the initial steps in the photodegradation of metolachlor. The loss of chorine is assumed to be initiated by absorption of photons where the chlorine forms MCA (*13*).

Figure 7 presents a suggested scheme of photodegradation of metolachlor, based on the six identified products

(**Figure 6**). The loss of the chlorine atom might be initiated by absorption of photons and result in formation of the intermediates 1 and 2, which proceed to compounds **10** and **4**. Cyclization of compound **10** results in the formation of compound **7**. The CH_2CH_3 group on the benzene ring in intermediate 2 may also undergo cyclization to form compounds **1**, **2**, and **14**.

LITERATURE CITED

(1) U.S. Environmental Protection Agency (EPA). *Pesticides Industry Sales and Usage 2000 and 2001 Market Estimates*; U.S. Government Printing Office: Washington, DC, 2004; www.epa.gov/oppbead1/pestsales.

(2) Seybold, C. A.; Mersie, W.; McNamee, C. Anaerobic degradation of atrazine and metolachlor and metabolite formation in wetland soil and water microcosms. *J. Environ. Qual.* **2001**, *31*, 1271−1277.

(3) Kochany, J.; Maguire, R. Sunlight photodegradation of metolachlor in water. *J. Agric. Food Chem.* **1994**, *42*, 406−412.

(4) Dinelli, G.; Accinelli, C.; Vicari, A.; Catizone, P. Comparison of the persistence of atrazine and metolachlor under field and laboratory conditions. *J. Agric. Food Chem.* **2000**, *48*, 3037−3043.

(5) Kolpin, D. W.; Barbash, J.; Gilliom, R. J. Occurrence of pesticides in shallow groundwater of the United States: Initial results from the National Water-Quality Assessment Program. *Environ. Sci. Technol.* **1998**, *32*, 558−566.

(6) Chesters, G.; Simsiman, G. V.; Levy, J.; Alhajjar, B. J.; Fathulla, R. N.; Harkin, J. M. Environmental fate of alachlor and metolachlor. *Rev. Environ. Contam. Toxicol*. **1989**, *110*, 1−74.

(7) World Health Organization (WHO). *Guidelines for Drinking-Water Quality*, 2nd ed.; WHO: Geneva, 1996; Vol. 2, Health criteria and other supporting information.

(8) Health Canada. *Guidelines for Canadian Drinking Water Quality—Summary Table*; Health Canada: Ottawa, Canada, 2006; www.healthcanada.gc.ca/waterquality.

(9) Liu, S. Y.; Freyer, A. J.; Bollag, J. M. Microbial dechlorination of the herbicide metolachlor. *J. Agric. Food Chem.* **1991**, *39*, 631−636.

(10) Kalkhoff, S. J.; Kolpin, D. W.; Thurman, E. Degradation of chloroacetanilides herbicides: The prevalence of sulfonic and oxanilic acid metabolites in Iowa groundwaters and surface waters. *Environ. Sci. Technol.* **1998**, *32*, 1738−1740.

(11) Acero, J. L.; Benitez, F. J.; Real, F. J.; Maya, C. Oxidation of acetamide herbicides in natural waters by ozone and by the combination of ozone/hydrogen peroxide: Kinetic study and process modeling. *Ind. Eng. Chem. Res.* **2003**, *42*, 5762−5769.

(12) Pignatello, J. J.; Sun, Y. F. Complete oxidation of metolachlor and methyl parathion in water by the photoassisted Fenton reaction. *Water Res.* **1995**, *29*, 1837−1844.

(13) Wilson, R. I.; Mabury, S. A. Photodegradation of metolachlor: Isolation, identification, and quantification of monochloroacetic acid. *J. Agric. Food Chem.* **2000**, *48*, 944−950.

(14) Mathew, R.; Khan, S. U. Photodegradation of metolachlor in water in the presence of mineral and organic constituents. *J. Agric. Chem. Chem*. **1996**, *44*, 3996−4000.

(15) Feigenbrugel, V.; Calve, S.; Mirabel, P. Temperature dependence of Henry's Law constants of metolachlor and diazinon. *Chemosphere* **2004**, *57*, 319−327.

(16) Lopez, A.; Bozzi, A.; Mascolo, G.; Kiwi, J. Kinetic investigation on UV and UV/ H_2O_2 degradation of pharmaceutical intermediates in aqueous solution. *J. Photochem. Photobiol., A* **2003**, *156*, 121−126.

(17) Cater, S. R.; Stefan, M. I.; Bolton, J. R.; Safarzadeh-Amirl, A. UV/H_2O_2 treatment of methyl *tert*-butyl ether in contaminated waters. *Environ Sci. Technol*. **2000**, *34*, 659−662.

(18) Einschlag, F.; Lopez, J.; Carlos, L.; Capparelli, A. Evaluation of the efficiency of photodegradation of nitroaromatics applying the UV/H_2O_2 technique. *Environ. Sci. Technol.* **2002**, *36*, 3936−3944.

(19) Sharpless, M. C.; Linden, K. G. Experimental and model comparisons of low- and medium-pressure Hg lamps for the direct and H_2O_2 assisted UV photodegradation of N-nitrosodimethylamine in simulated drinking water. *Environ. Sci. Technol*. **2003**, *37*, 1933−1940.

(20) Rosenfeldt, E. J.; Linden, K. G. Degradation of endocrine disrupting chemicals bisphenol A, ethinyl estradiol, and estradiol during UV photolysis and advanced oxidation processes. *Environ. Sci. Technol.* **2004**, *38*, 5476−5483.

(21) Standard Methods. In *Standard Methods for the Examination of Water and Wastewater*, 20th ed.; Clesceri, L. S., Greenberg, A. E., Eaton, A. D., Eds.; American Public Health Association: Washington, DC, 1998.

(22) Klassen, N.; Marchington, D.; McGowan, H. C. C. H_2O_2 determination by the I_3^- method and $KMnO_4$ titration. *Anal. Chem.* **1994**, *66*, 2921−2925.

(23) Schwarzenbach, R. P.; Gschwend, P.; Imboden, D. M. *Environmental Organic Chemistry*; Wiley-Interscience, John Wiley and Sons: New York, 1993.

(24) Benitez, F. J.; Acero, J. L.; Real, F. J.; Maya, C. Modeling of photooxidation of acetamide herbicides in natural waters by UV radiation and the combinations UV/ H_2O_2 and UV/O_3. *J. Chem. Technol. Biotechnol*. **2004**, *79*, 987−997.

(25) Glaze, W.; Lay, Y.; Kang, J. W. Advanced oxidation processes. A kinetic model for the oxidation of 1,2-dibromo-3-chloropropane in water by the combination of hydrogen peroxide and UV radiation. *Ind. Eng. Chem. Res.* **1995**, *34*, 2314−2323.

(26) Stefan, M. I.; Hoy, A. R.; Bolton, J. R. Kinetics and mechanism of the degradation and mineralization of acetone in dilute aqueous solution sensitized by the UV photolysis of hydrogen peroxide. *Environ. Sci. Technol.* **1996**, *30*, 2382−2390.

(27) Behnajady, M. A.; Modirshahla, N.; Shokri, M. Photodestruction of acid orange 7 (AO7) in aqueous solutions by UV/H_2O_2: Influence of operational parameters. *Chemosphere* **2004**, *55*, 129−134.

(28) Buxton, G.; Greenstock, C. L.; Helman, W. P.; Ross, A. B. Critical review of rate constants for reactions of hydrated electrons, hydrogen atoms and hydroxyl radicals (OH/O^-) in aqueous solution. *J. Phys. Chem. Ref. Data* **1998**, *17*, 513−886.

(29) Palm, W. U.; Kopetzky, R.; Ruck, W. OH-radical reactivity and direct photolysis of triphenyltin hydroxide in aqueous solution. *J. Photochem. Photobiol., A* **2003**, *156*, 105−114.

(30) Allen, J. M.; Lucas, S.; Allen, K. Formation of hydroxyl radicals (OH) in illuminated surface waters contaminated with acid mine drainage. *Environ. Toxicol. Chem*. **1996**, *15*, 107−113.

(31) Vogna, D.; Marotta, R.; Andreozzi, R.; Napolitano, A.; d'Ischia, M. Kinetic and chemical assessment of the UV/H_2O_2 treatment of antiepileptic drug carbamazepine. *Chemosphere* **2004**, *54*, 497−505.

(32) Juang, L.; Tseng, D.; Lee, J. F. Photolytic mechanism of monochlorobenzene in an aqueous UV/ H_2O_2 system. *Chemosphere* **1998**, *36*, 1187−1199.

(33) Hoigne, J.; Bader, H. Ozonation of water: "Oxidation-competition values" of different types of waters used in Switzerland. *Ozone Sci. Eng*. **1979**, *1*, 357−372.

(34) McGahen, L. L.; Tiedje, J. M. Metabolism of 2 new acylanilide herbicides, antor herbicide (H-22234) and dual (metolachlor) by soil fungus chaetomium-globosum. *J. Agric. Food Chem.* **1978**, *26*, 414−419.

Received for review December 11, 2006. Revised manuscript received March 2, 2007. Accepted March 13, 2007. The U.S. Environmental Protection Agency through its Office of Research and Development funded and collaborated in the research described here under CR-829412-01-1 to Duke University. It has not been subject to Agency review and therefore does not necessarily reflect the views of the Agency. No official endorsement should be inferred.

JF0635762